

The Aharonov-Bohm effect in mesoscopic Bose-Einstein condensates

Tobias Haug,¹ Hermanni Heimonen,¹ Rainer Dumke,^{1,2,3} Leong-Chuan Kwek,^{1,3,4,5} and Luigi Amico^{1,3,6,7,8}

¹Centre for Quantum Technologies, National University of Singapore, 3 Science Drive 2, Singapore 117543, Singapore

²Division of Physics and Applied Physics, Nanyang Technological University, 21 Nanyang Link, Singapore 637371, Singapore

³MajuLab, CNRS-UNS-NUS-NTU International Joint Research Unit, UMI 3654, Singapore

⁴Institute of Advanced Studies, Nanyang Technological University, 60 Nanyang View, Singapore 639673, Singapore

⁵National Institute of Education, Nanyang Technological University, 1 Nanyang Walk, Singapore 637616, Singapore

⁶Dipartimento di Fisica e Astronomia, Via S. Sofia 64, 95127 Catania, Italy

⁷CNR-MATIS-IMM & INFN-Sezione di Catania, Via S. Sofia 64, 95127 Catania, Italy

⁸LANEF 'Chaire d'excellence', Université Grenoble-Alpes & CNRS, F-38000 Grenoble, France

(Dated: September 13, 2022)

The Aharonov-Bohm, and its dual, the Aharonov-Casher effect have been extremely fruitful in physics and, nowadays, they are of central importance for quantum technologies. Here, we study the Aharonov-Bohm effect for a Bose-Einstein condensate propagating out of equilibrium along a mesoscopic ring-shaped laser light potential, pierced by an effective magnetic flux. We found how the system experiences a subtle crossover between physical regimes dominated by pronounced interference patterns and others in which the Aharonov-Bohm effect is effectively washed out. We propose various applications for this system.

The Aharonov-Bohm effect is one of the most striking manifestations of quantum mechanics: Due to phase shifts in the wave function, specific interference effects arise when charged particles enclose a region with a non vanishing magnetic field[1]. This effect has important implications in foundational aspects of quantum physics[1–4] and many-body quantum physics[5–11]. The Aharonov-Bohm effect has been influential in many fields of physical sciences, like mesoscopic physics, quantum electronics and molecular electronics[12–15], with remarkable applications enabling quantum technologies[16–21].

An electronic fluid confined to a ring-shaped wire pierced by a magnetic flux is the typical configuration employed to study the Aharonov-Bohm effect. In this way, a matter-wave interferometer is realized: The current through the ring-shaped quantum system displays characteristic oscillations depending on the imparted magnetic flux. Neutral particles with magnetic moments display similar interference effects[22].

A new perspective to study the transport through small and medium sized quantum matter systems has been demonstrated recently in ultracold atoms[23–25]: In such systems, it is possible for the first time to manipulate and adjust the carrier statistics, particle-particle interactions and spatial configuration of the circuit. Such flexibility is very hard, if not impossible, to achieve using standard realizations of mesoscopic systems. For this scenario Atomtronics has been put forward[26, 27].

In this paper, we study the Aharonov-Bohm effect in a mesoscopic ring-shaped bosonic condensate pierced by a synthetic magnetic flux[28]: The bosonic fluid is injected from a ‘source’ lead, propagates along the ring, and it is collected in a ‘drain’ lead. In this way, we provide the atomtronic counterpart of an iconic problem in mesoscopic physics[12, 13], with far reaching implications over the years in the broad area of physical science[5–11, 16–21]. We also observe that such a system provides one of the elementary components

of atomtronic integrated circuits under current experimental study[29]. We analyse the non-equilibrium dynamics of the system by quenching the particles spatial confinement; our study is combined with the analysis of the out-of-equilibrium dynamics triggered by driving the current through suitable baths attached to the system. We find that, depending on the ring-lead coupling, boson-boson interactions and particle statistics, the system displays qualitatively distinct non-equilibrium regimes characterized by different response of the interference pattern established by the effective gauge field. We see, in particular, that the bosonic system displays distinctively different features compared with the corresponding fermionic system. Finally, we explore our findings for possible applications for the realization of new atomtronic quantum devices.

The system dynamics– The Bose-Hubbard Hamiltonian

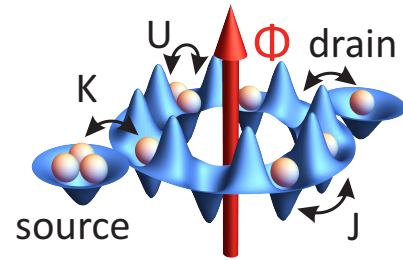


FIG. 1. Atomtronic setup consisting of a superfluid condensate in a ring lattice with two attached leads. The dynamics is controlled by Aharonov-Bohm flux Φ and ring-lead coupling K . Particles tunnel between ring sites with rate J and particles interact on-site with strength U .

$\mathcal{H} = \mathcal{H}_r + \mathcal{H}_l$ describes the system consisting of a ring with an even number of lattice sites L and two leads (see Fig. 1).

The ring is given by

$$\mathcal{H}_r = - \sum_{j=0}^{L-1} \left(J e^{i2\pi\Phi/L} \hat{a}_j^\dagger \hat{a}_{j+1} + \text{H.C.} \right) + \frac{U}{2} \sum_{j=0}^{L-1} \hat{n}_j (\hat{n}_j - 1), \quad (1)$$

where \hat{a}_j and \hat{a}_j^\dagger are the annihilation and creation operator at site j , $\hat{n}_j = \hat{a}_j^\dagger \hat{a}_j$ is the particle number operator, J is the intra-ring hopping, U is the on-site interaction between particles and Φ is the total flux through the ring. Periodic boundary conditions are applied: $\hat{a}_L^\dagger = \hat{a}_0^\dagger$.

The two leads dubbed source (S) and drain (D) consist of a single site each, which are coupled symmetrically at opposite sites to the ring with coupling strength K . In both of them, local potential energy and on-site interaction are set to zero as the leads are considered to be large with low atom density. The lead Hamiltonian is $\mathcal{H}_l = -K(\hat{a}_S^\dagger \hat{a}_0 + \hat{a}_D^\dagger \hat{a}_{L/2} + \text{H.C.})$, where \hat{a}_S^\dagger and \hat{a}_D^\dagger are the creation operators of source and drain respectively.

The system is initially prepared with all particles in the source and the dynamics is strongly affected by the lead-ring coupling. We calculate the state at time t with $|\Psi(t)\rangle = e^{-iHt} |\Psi(0)\rangle$. We investigate the expectation value of the density in source and drain over time, which for the source is calculated as $n_{\text{source}}(t) = \langle \Psi(t) | \hat{a}_S^\dagger \hat{a}_S | \Psi(t) \rangle$ and similar for the drain. We point out that, by construction, our approach is well defined for the whole cross-over ranging from the weak to strong leads-system coupling (this feature should be contrasted with the limitations of traditional approaches for interacting particles mostly valid for the regime of weak leads-system coupling).

In the weak-coupling regime $K/J \ll 1$, the lead-ring tunneling is slow compared to the dynamics inside the ring. In this regime, the condensate mostly populates the drain and source, leaving the ring nearly empty. As a result, the scattering due to on-site interaction U has a negligible influence on the dynamics. The transfer rate through the ring is strongly

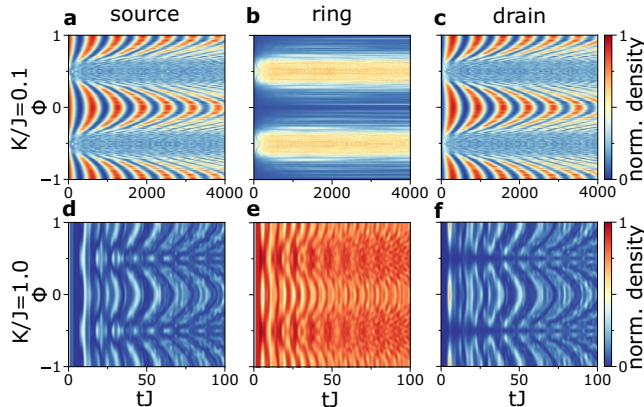


FIG. 2. Time evolution of density in source **a,d**), ring **b,e**) and drain **c,f**) plotted against flux Φ . **a,b,c**) weak ring-lead coupling $K/J = 0.1$ (on-site interaction $U/J = 5$). **d,e,f**) strong ring-lead coupling $K/J = 1$ ($U/J = 0.2$). The number of ring sites is $L = 14$ with $N_p = 4$ particles initially in the source. The density in the ring is $n_{\text{ring}} = 1 - n_{\text{source}} - n_{\text{drain}}$.

influenced by interference, giving rise to regular patterns and a pronounced Aharonov-Bohm effect at $\Phi = 0$ (Fig.2a,b,c). With increasing Φ the oscillation becomes faster and the ring

populates, resulting in increased scattering and washed-out density oscillations.

In the strong-coupling regime $K/J \approx 1$, the lead-ring and the intra-ring dynamics are characterized by the same frequency and cannot be treated separately. We find that the crossover from weak to strong coupling regime is marked by the appearance of additional frequency modes in the time evolution of the density (see also supplementary material). Thus, in the strong coupling regime, we see a superposition of many oscillation frequencies, and after a short time the condensate is evenly spread both in the leads and in the ring potential (Fig.2d,e,f). The density in the ring is large and particle scattering affects the dynamics by washing out the oscillations. Close to $\Phi = 0.5$, the oscillation between source and drain slows down, especially for weak interaction, due to destructive interference.

For two atoms, the ring spectrum can be derived analytically [30] in terms of scattering (real valued relative quasi-momentum k) and bound states (imaginary k). The bound states have only half the flux quantum compared to single atoms (like Cooper-pairs) and therefore interfere constructively when propagating through the ring at the degeneracy point. For very weak interaction, the oscillations in a simplified model of a ring without leads can be calculated from the energy difference of bound and scattering states at the edge of the Brillouin zone. We find that the analytic results matches the main oscillation period of the full numerical calculation.

We find that the dynamics is affected by the parity in half of the number of ring sites $L/2$, which is especially pronounced in the weak-coupling regime. In Fig.3, the density in source and drain is plotted against Φ for odd ($L/2 = 3, 5, 7, \dots$) and even parity ($L/2 = 2, 4, 6, \dots$) for $K/J = 0.1$. Both flux dependence and time scales differ widely for the two parities. With a similar logic of the tunneling through quantum dots, we can understand such parity effects in terms of ring-lead resonant and off-resonant coupling[31, 32]. We point out, however, that the parity effect leads to a phenomenology that is very specific for our system. Off-resonant coupling is characterized by regular, slow oscillations between source and drain and a small ring population. Resonant coupling implies faster oscillation, but a large ring population. Such conditions are substantially affected by the interplay between interaction U and Φ . The flux Φ modifies the energy eigenmodes of the ring, bringing them in and out of resonance with the leads. Interaction U can wash out the oscillations between source and drain when the ring population is large. For odd parity, we find that both resonant and off-resonant coupling contributes. Close to $\Phi = 0$ the off-resonant coupling dominates. Due to the small ring population, the interaction (we checked up to $U/J = 5$) has only a minor effect on the dynamics. Close to $\Phi = 0.5$, resonant ring modes become dominant, and the oscillations become faster and tend to be washed out due to a higher ring population. For even parity only resonant coupling is possible. Close to $\Phi = 0$, ring modes are on resonance. Thus, we see faster oscillation compared to the odd parity, although they are washed out by interactions. For increasing Φ , how-

ever, the ring modes move out of resonance, and due to the absence of off-resonant coupling, the transfer is suppressed (detailed derivation in supplementary materials). These parity effects are less visible for strong coupling or many ring sites as the level spacing between ring modes diminishes and many ring modes come into resonance, washing out the difference between the parities.

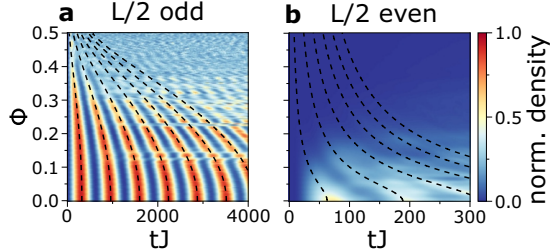


FIG. 3. Density in drain against flux Φ and parity in number of ring sites odd **a)** $L/2 = 7$ ($U/J = 3$) and even **b)** $L/2 = 8$ ($U/J = 1$). Simulation with $N_p = 4$ and weak coupling ($K/J = 0.1$). The structures around $\Phi = 0.15$ for odd parity are many-body resonances[33]. Dashed line shows analytic derived oscillation period (**a** Eq.10 and **b** Eq.3 in the supplementary material).

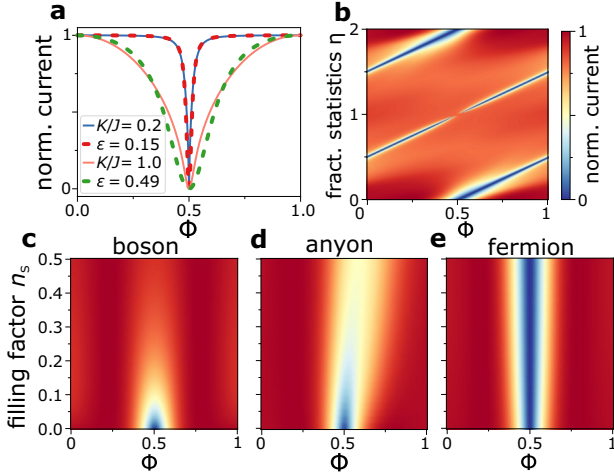


FIG. 4. Steady-state currents. **a)** Solid lines: steady-state current we obtained applying the method presented in [34, 35] for non-interacting particles with $L = 100$. Dashed lines: a fit ($\epsilon = \{0.15, 0.49\}$) with the transmission equations derived by Büttiker et al.[13]. **b)** Steady-state current for infinite on-site interaction in both leads and ring plotted against flux Φ and fractional statistics η ($\eta = \{0, 2\}$ non-interacting fermions, $\eta = 1$ hard-core bosons, else anyons) for strong source-drain imbalance. The reservoirs obey the Pauli principle with $f = 1$, $\Gamma = 1/2$. The number of ring sites is $L/2 = 3$ and the ring-lead coupling is $K/J = 1$. At the transition to bosons, there is a discontinuity in the current. **c-e)** Steady state current for hard-core bosons, anyons ($\eta = 0.25$) and fermions plotted against flux and the filling factor n_s . The reservoirs can have multiple particles per state and have a small particle number imbalance between source and drain with $n_s - n_D = 0.01$. The current is normalized to one for each value of filling independently.

Open system– To study the properties of a filled

ring, in Fig.4 we couple particle reservoirs with the leads to drive a current through the now open system. We model it using the Lindblad master equation $\frac{\partial \rho}{\partial t} = -\frac{i}{\hbar} [H, \rho] - \frac{1}{2} \sum_m \{ \hat{L}_m^\dagger \hat{L}_m, \rho \} + \sum_m \hat{L}_m \rho \hat{L}_m^\dagger$ for the reduced density matrix (tracing out the baths) [36]. The bath-lead coupling is assumed to be weak and within the Born-Markov approximation. We consider two types of reservoirs: First, reservoirs allowing multiple particles per state $L_1 = \sqrt{\Gamma n_S} \hat{a}_S^\dagger$, $L_2 = \sqrt{\Gamma(n_S + 1)} \hat{a}_S$, $L_3 = \sqrt{\Gamma n_D} \hat{a}_D^\dagger$ and $L_4 = \sqrt{\Gamma(n_D + 1)} \hat{a}_D$ (n_S (n_D) is the density of the source (drain) site if uncoupled to the ring). Second, reservoirs with a single particle per state and (which enforces the Pauli-principle) $L_1 = \sqrt{\Gamma/2(1+f)} \hat{a}_S^\dagger$, $L_2 = \sqrt{\Gamma/2(1-f)} \hat{a}_S$, $L_3 = \sqrt{\Gamma/2(1-f)} \hat{a}_D^\dagger$ and $L_4 = \sqrt{\Gamma/2(1+f)} \hat{a}_D$ (f characterizes the atom imbalance between source and drain reservoirs, with $f = 1$ being the source reservoir full and the drain reservoir empty). We solve the equations for the steady-state of the density matrix $\frac{\partial \rho_{SS}}{\partial t} = 0$ numerically[37]. The current operator is $j = -iK(\hat{a}_S^\dagger \hat{a}_0 - \hat{a}_0^\dagger \hat{a}_S)$. The expectation value is calculated as $\langle j \rangle = \text{Tr}(j \rho_{SS})$. We generalize the particle statistics with the parameter η ($\eta = \{0, 2\}$ fermions, $\eta = 1$ bosons, else anyons) using the transformation $\hat{a}_n^\dagger \rightarrow \hat{a}_n^\dagger \prod_{j=n+1}^L e^{i\pi(1-\eta)\hat{n}_j}$ [38–40]. For vanishing particle-particle interactions, we found the matching conditions between the equilibrium scattering-based results of Büttiker et al.[13] and non-equilibrium steady state currents – Fig.4 a). Next, we enforce the Pauli-principle ($U = \infty$) in both leads and ring and vary the particle statistics and the average number of particles in the system (filling factor). Fermions are then non-interacting, while anyons and bosons interact more strongly with increasing filling. We found that the type of particle (Boson, fermion, anyon as defined in [38]) and inter-particle interaction has a profound influence on the Aharonov-Bohm effect–Fig.4 b) - e). While non-interacting particles react strongly to an applied flux, interacting bosons have only weak dependence on the flux. Fermions have zero current at the degeneracy point, while anyons have a specific point with minimal current, which depends on the reservoir properties. With increasing filling of hard-core bosons, scattering increases and Aharonov-Bohm effect vanishes. For fermions, it is independent of the particle density and for anyons it depends on the reservoir properties. Remarkably, for interacting bosons in the strong coupling regime the Aharonov-Bohm effect is effectively suppressed[41], whereas some structure in the transmission is observed for weak coupling. In summary, the Aharonov-Bohm effect in the mesoscopic regime does experience a non-trivial cross-over as a function of interaction, carrier statistics and the ring-lead coupling strength.

Applications– Here we present possible applications based on the physics discussed above. We study the applications for the closed ring-lead configuration, with the atoms initially in the source.

As first application, we study the atomtronic counterpart of the dc-SQUID: We change the local potential by Δ at two single sites in the ring symmetrically in the upper and lower half.

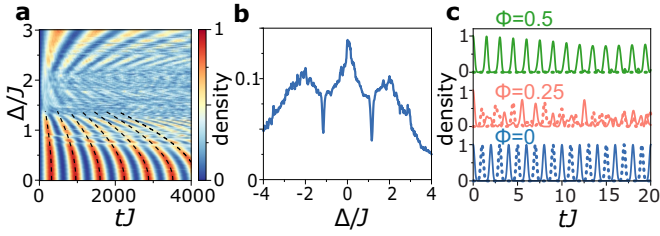


FIG. 5. **a)** Density in drain plotted against two potential barriers placed symmetrically in both arms of the ring with depth Δ . $L = 14$, $N_p = 4$, $K/J = 0.1$ and $U/J = 3$. Dashed line indicates a fit with the analytic formula for the oscillation period used for the flux dependence in Fig.3a,b (Supplementary material Eq.10, replace Φ with $\Delta/(2J)$). **b)** Average density in drain integrated over a time $t = 10000/J$ for a potential well with depth Δ in one arm of the ring. Interference effects cause minima in transmission rate for certain values of Δ . $L = 14$, $N_p = 4$, $K/J = 1$ and $U/J = 0.1$. **c)** Density in source (solid) and drain (dashed) for the perfect state transfer protocol with $U/J = 0$ and $L = 14$. With this protocol, particles oscillate between source and drain with period $t = 2$. From bottom to top $\Phi = \{0, 0.25, 0.5\}$.

To achieve this, we add the following part to the Hamiltonian $\mathcal{H}_{\text{imp}} = \Delta(\hat{n}_{[L/4]} + \hat{n}_{[3L/4]})$. The time-evolution depending on Δ is shown in Fig.5a,b. The potential barrier modifies the transfer rate to the drain in a quantitatively similar way as the Aharonov-Bohm flux. However, no destructive interference is observed. This indicates that the barrier influences the dynamics only by scattering incoming particles, but does not imprint a phase shift. However, by adjusting Δ we can control the source-drain transfer rate in a similar fashion as the flux.

As a second application, we study the propagation through a quantum dot like structure[31, 42]. This time, the local potential is changed by adding a potential well on one arm of the ring $\mathcal{H}_{\text{qd}} = \Delta \sum_{j=0}^{(L-6+\text{mod}(L,4))/2} \hat{n}_j$. We found that distinct transmission minima are displayed (see Fig.5c). Such results indicate that the particle acquires a phase difference while traveling through the ring. This device could realize a switch by changing Δ around the transmission minima, or alternatively a simulator for quantum dots.

Finally, we investigate the Perfect State Transfer protocol, where particles move from source to drain and vice-versa without dispersion at a fixed rate ([43]). The coupling parameters are $J_n = \frac{\pi}{2} J \sqrt{s_n} \sqrt{n(L_0 - n)}$, where n is numeration of the coupling from source to drain, $L_0 = L/2 + 3$ the number of sites on the shortest path between source and drain, and s_n secures the Kirchhoff's law. We set $s_n = 1$ everywhere except at the two ring sites which are coupled directly to the leads: There, the coupling of those sites to the neighboring two ring sites is $s_n = 1/2$. The flux dependence of the time evolution of the density for $U = 0$ is shown in Fig.5d. At $\Phi = 0$ we observe that the density in source and drain oscillates at a constant rate with close to unit probability. Depending on interaction and particle number, the fidelity of the transport remains at unity or decreases. We will study this interesting effect in a future publication. In contrast to weak coupling,

the particles move as a wave packet inside the ring. By tuning the flux, the drain density can be controlled and transmission to the drain becomes zero at the degeneracy point. The setup with perfect state transfer could realize a switch or atomtronic quantum interference transistors: By changing the flux, perfect transmission is changed into perfect reflection. We propose to use the high control over the dynamics to create an atomic version of a Elitzur-Vaidman bomb tester, the hallmark example of interaction-free measurement[44]. The system is prepared with a single particle, the flux set to the degeneracy point and a bomb, which is triggered when a particle passes through one specific arm of the ring. Without the bomb, the Aharonov-Bohm effect prevents the particle from reaching the drain. Only if there is a bomb and the particle has not been triggered it, the particle reaches the drain with unit probability due to the perfect state transfer. This setup has a 50% chance to detect the bomb without detonating it, improving from the 33% efficiency of the photonic implementation.

Our results can be relevant in other contexts of quantum technology, beyond ultracold atoms[45].

Conclusions. We studied the non equilibrium transmission through an Aharonov-Bohm mesoscopic ring. By quenching the spatial confinement, the dynamics is strongly affected by the leads-ring coupling, the parity of the ring sites, and the interaction of the atoms. By combining our analysis with the study of the non-equilibrium steady states in an open system, we find that the Aharonov-Bohm effect is washed out for interacting bosons. Finally, we have analyzed the possible implications of our study to conceive new quantum atomtronic devices. We believe our study will be instrumental to bridge cold-atom and mesoscopic physics. Most of the physics we studied here could be explored experimentally with the current know-how in quantum technology.

Acknowledgments. The Grenoble LANEF framework (ANR-10-LABX-51-01) is acknowledged for its support with mutualized infrastructure. We thank National Research Foundation Singapore and the Ministry of Education Singapore Academic Research Fund Tier 2 (Grant No. MOE2015-T2-1-101) for support.

-
- [1] Y. Aharonov and D. Bohm, Phys. Rev. **115**, 485 (1959).
 - [2] S. Olariu and I. I. Popescu, Rev. Mod. Phys. **57**, 339 (1985).
 - [3] L. Vaidman, Phys. Rev. A **86**, 040101 (2012).
 - [4] A. J. Leggett, Progr. Theoret. Phys. Suppl. **69**, 80 (1980).
 - [5] A. Lobos and A. Aligia, Phys. Rev. Lett. **100**, 016803 (2008).
 - [6] F. Marquardt and C. Bruder, Phys. Rev. B **65**, 125315 (2002).
 - [7] J. Rincón, K. Hallberg, and A. Aligia, Phys. Rev. B **78**, 125115 (2008).
 - [8] J. Rincón, A. Aligia, and K. Hallberg, Phys. Rev. B **79**, 035112 (2009).
 - [9] P. Shmakov, A. Dmitriev, and V. Y. Kachorovskii, Phys. Rev. B **87**, 235417 (2013).
 - [10] O. Hod, R. Baer, and E. Rabani, Phys. Rev. Lett. **97**, 266803 (2006).
 - [11] E. Jagla and C. Balseiro, Phys. Rev. Lett. **70**, 639 (1993).

- [12] Y. Gefen, Y. Imry, and M. Y. Azbel, Phys. Rev. Lett. **52**, 129 (1984).
- [13] M. Büttiker, Y. Imry, and M. Y. Azbel, Phys. Rev. A **30**, 1982 (1984).
- [14] R. A. Webb, S. Washburn, C. Umbach, and R. Laibowitz, Phys. Rev. Lett. **54**, 2696 (1985).
- [15] A. Nitzan and M. A. Ratner, Science **300**, 1384 (2003).
- [16] N. Byers and C. Yang, Phys. Rev. Lett. **7**, 46 (1961).
- [17] F. Bloch, Phys. Rev. **166**, 415 (1968).
- [18] L. Gunther and Y. Imry, Solid State Commun. **7**, 1391 (1969).
- [19] A. Bachtold, C. Strunk, J.-P. Salvetat, J.-M. Bonard, L. Forró, T. Nussbaumer, and C. Schönenberger, Nature **397**, 673 (1999).
- [20] U. C. Coskun, T.-C. Wei, S. Vishveshwara, P. M. Goldbart, and A. Bezryadin, Science **304**, 1132 (2004).
- [21] D. M. Cardamone, C. A. Stafford, and S. Mazumdar, Nano Lett. **6**, 2423 (2006).
- [22] Y. Aharonov and A. Casher, Phys. Rev. Lett. **53**, 319 (1984).
- [23] D. Papoular, L. Pitaevskii, and S. Stringari, Phys. Rev. Lett. **113**, 170601 (2014).
- [24] A. Li, S. Eckel, B. Eller, K. E. Warren, C. W. Clark, and M. Edwards, Phys. Rev. A **94**, 023626 (2016).
- [25] S. Krinner, D. Stadler, D. Husmann, J.-P. Brantut, and T. Esslinger, Nature **517**, 64 (2015).
- [26] L. Amico and A. M. G. Boshier, in *R. Dumke, Roadmap on quantum optical systems*, Vol. 18 (Journal of Optics, 2016) p. 093001.
- [27] L. Amico, G. Birkel, M. Boshier, and L.-C. Kwek, *New Journal of Physics* **19**, 020201 (2017).
- [28] J. Dalibard, F. Gerbier, G. Juzeliūnas, and P. Öhberg, Rev. Mod. Phys. **83**, 1523 (2011).
- [29] C. Ryu and M. G. Boshier, *New Journal of Physics* **17**, 092002 (2015).
- [30] M. Valiente and D. Petrosyan, J. Phys. B **41**, 161002 (2008).
- [31] J. Wu, B.-L. Gu, H. Chen, W. Duan, and Y. Kawazoe, Phys. Rev. Lett. **80**, 1952 (1998).
- [32] L. Glazman and M. Pustilnik, in *New directions in mesoscopic physics (towards nanoscience)* (Springer, 2003) pp. 93–115.
- [33] M. Sturm, M. Schlosser, R. Walser, and G. Birkel, arXiv:1705.01271.
- [34] T. Prosen, New J. Phys. **10**, 043026 (2008).
- [35] C. Guo and D. Poletti, Phys. Rev. A **95**, 052107 (2017).
- [36] H.-P. Breuer and F. Petruccione, *The theory of open quantum systems* (Oxford University Press on Demand, 2002).
- [37] C. Guo and D. Poletti, Phys. Rev. B **96**, 165409 (2017).
- [38] L. Amico, A. Osterloh, and U. Eckern, Phys. Rev. B **58**, R1703 (1998).
- [39] T. Keilmann, S. Lanzmich, I. McCulloch, and M. Roncaglia, Nat. Commun. **2**, 361 (2011).
- [40] S. Greschner and L. Santos, Phys. Rev. Lett. **115**, 053002 (2015).
- [41] A. Tokuno, M. Oshikawa, and E. Demler, Phys. Rev. Lett. **100**, 140402 (2008).
- [42] A. L. Yeyati and M. Büttiker, Phys. Rev. B **52**, R14360 (1995).
- [43] L. Dai, Y. Feng, and L. Kwek, J. Phys. A Math. Theor. **43**, 035302 (2009).
- [44] A. C. Elitzur and L. Vaidman, Found. Phys. **23**, 987 (1993).
- [45] P. Roushan, C. Neill, A. Megrant, Y. Chen, R. Babbush, R. Barends, B. Campbell, Z. Chen, B. Chiaro, A. Dunsworth, *et al.*, Nat. Phys. **13**, 146 (2017).

Appendix: I. Time dynamics

Appendix: Analytic results on the time-dynamics of non-interacting particles

In this section, we derive analytic results for the time evolution in the dynamics between source and drain. To investigate the Hamiltonian, it is convenient to write the ring Hamiltonian in Fourier space (for $U = 0$)

$$\mathcal{H}_t = \sum_{j=0}^{L-1} -2J \cos\left(\frac{2\pi}{L}(j - \Phi)\right) \hat{b}_j^\dagger \hat{b}_j + \sum_{j=0}^{L-1} \frac{K}{\sqrt{L}} \left(\hat{a}_S^\dagger \hat{b}_j + (-1)^j \hat{a}_D^\dagger \hat{b}_j + \text{H.C.} \right), \quad (\text{A.2})$$

where \hat{b}_j (\hat{b}_j^\dagger) the Fourier transform of the annihilation (creation) operator of the ring.

In the following, we assume that all the particles are initially loaded into the source. We investigate the dynamics for weak coupling $K \ll J$ or for small number of ring sites L . The time evolution is governed by the eigenmodes $|\Psi_j\rangle$ with energy E_j . It is given by $|\Psi(t)\rangle = \sum_j e^{-iE_j t} |\Psi_j\rangle \langle \Psi_j | \Psi(0)\rangle$. We define the coefficient of the overlap between eigenstate and initial condition $A_j = \langle \Psi_j | \Psi(0)\rangle$. Due to the symmetry of the system, the spectrum has pairs of eigenvalues $\pm E_j$. We find that the absolute value of A_j is the same for these pairs (the sign depends on the parity), in both source and drain. Using these properties, we can write the dynamics for the density in source n_S for each eigenvalue pair, where j is summed over $L/2 + 1$ eigenvalue pairs in ascending order of the eigenvalues

$$n_S(t) = \left| \sum_{j \in \text{pairs}} \cos(E_j t) |A_j|^2 \right|^2$$

and the drain density n_D for odd parity

$$n_D(t) = \left| \sum_{j \in \text{pairs}} (-1)^j \sin(E_j t) |A_j|^2 \right|^2$$

and for even parity

$$n_D(t) = \left| \sum_{j \in \text{pairs}} (-1)^j \cos(E_j t) |A_j|^2 \right|^2.$$

In the weak coupling limit $K \ll J$ or for small number of ring sites L , the dynamics can be described by an effective, reduced system, consisting of source, drain and a small number of ring eigenmodes L_0 . With above equations, the dynamics is then given by the sum over the $L_0/2 + 1$ eigenmode pairs of the reduced system.

We justify this method as follows: Initially, all particles are prepared in the source and a total energy $E = 0$ (we assume that source and drain have zero potential energy). Source and

drain are coupled via the ring eigenmodes. Coupling is most efficient if the energy difference between the modes is small, thus the leads will couple mainly to the ring eigenmodes with energy close to the leads.

We identify two mechanism for transport through the ring: Firstly, resonant coupling to ring eigenmodes with energies close to that of the uncoupled leads. A similar concept is known as resonant tunneling in quantum dots. Secondly, off-resonant coupling enhanced by interference via all ring modes with energies not too close to the leads. Which mechanism is important depends on L and can be grouped into two distinct parities $L/2$ even and odd. For even parity, off-resonant coupling is not possible as it turns out the ring modes destructively interfere for any value of Φ . Thus, here transport is dominated by resonant coupling to ring eigenmodes $E \approx 0$. For odd parity, both mechanisms contribute. Here, for $\Phi \approx 0$, off-resonant coupling is dominant as there are no ring modes close to $E = 0$, while for $\Phi \approx \frac{1}{2}$ resonant coupling is dominant as there are two ring modes on resonance at $E = 0$. The difference in both parities arises from two effects: First, there are different eigenmode distributions. For example, for even parity and $\Phi = 0$ there are two ring modes with eigenvalue zero, whereas for odd parity this is not the case. For $\Phi = 0.5$, the opposite is true, e.g. odd parity has two ring modes with zero energy, whereas even parity has not.

The second contribution is the interference of ring modes at the ring-drain coupling. The eigenvalues can be grouped into pairs with the same absolute value, but opposite sign $\pm E$. They have the momentum mode number $n_- = n$ and $n_+ = n + \frac{L}{2}$. As seen in Eq.A.2, the sign of the ring-drain coupling depends on the momentum mode number. For even parity, an eigenvalue pair $\pm E$ has the same sign for the ring-drain coupling, whereas for odd the coupling for the two eigenvalues of the pair has opposite signs. This has a profound effect on the dynamics. For even parity, the eigenmode pair $\pm E$ will interfere destructively in the drain, while for odd constructively. This effect is independent of Φ . Note that when the ring modes couple strongly with the leads, the interference condition is relaxed (as the ring modes hybridize with source and drain). Thus, this argument is only strictly valid for off-resonant coupling. Both descriptions break down in the strong-coupling limit and for a large number of sites as more and more ring eigenmodes couple to the leads as the energy spacing between ring modes decreases.

Next, we describe how to calculate the eigenvalues of ring-lead system. We write down the eigenvalue equation with the Hamiltonian of Eq.A.2 for noninteracting particles $\hat{H}|\Psi\rangle = E|\Psi\rangle$ for an arbitrary eigenstate $|\Psi\rangle = \alpha_S|S\rangle + \alpha_D|D\rangle + \sum_{n=0}^{L-1} \alpha_n|n\rangle$, where α_S is the coefficient of the source site, α_D of the drain, and α_n of ring eigenmode n . We get $L + 2$

equations for the coefficients

$$\begin{aligned} E\alpha_S &= \frac{K}{\sqrt{L}} \sum_{n=0}^{L-1} \alpha_n \\ E\alpha_D &= \frac{K}{\sqrt{L}} \sum_{n=0}^{L-1} (-1)^n \alpha_n \\ E\alpha_n &= -2J \cos\left(\frac{2\pi(n-\Phi)}{L}\right) \alpha_n + \frac{K}{\sqrt{L}} (\alpha_S + (-1)^n \alpha_D). \end{aligned}$$

We insert the equations for α_n into the source and drain equations

$$\begin{aligned} E\alpha_S &= \frac{K^2}{2JL} \sum_{n=0}^{L-1} \frac{\alpha_S + (-1)^n \alpha_D}{\frac{E}{2J} + \cos\left(\frac{2\pi(n-\Phi)}{L}\right)} \\ E\alpha_D &= \frac{K^2}{2JL} \sum_{n=0}^{L-1} \frac{(-1)^n \alpha_S + \alpha_D}{\frac{E}{2J} + \cos\left(\frac{2\pi(n-\Phi)}{L}\right)}. \end{aligned} \quad (\text{A.3})$$

Using these two equations as starting point, we can make approximations. We define $\tilde{K} = K/J$.

For resonant coupling, we keep only the dominant terms of the sum in Eq.A.3. E.g. for odd parity and $\Phi \approx 0.5$ they are $n = \frac{L+2}{4}$ and $n = \frac{3L+2}{4}$, and for even parity with $\Phi \approx 0$ $n = \frac{L}{4}$ and $n = \frac{3L}{4}$. The resulting eigenvalues for even parity are

$$E = 0, \quad E/J = 2 \sqrt{\sin\left(\frac{2\pi\Phi}{L}\right)^2 + \left(\frac{\tilde{K}}{\sqrt{L}}\right)^2}, \quad (\text{A.4})$$

and for odd

$$E_{\pm}/J = \sin\left(\frac{2\pi(\Phi - 0.5)}{L}\right) \pm \sqrt{\sin\left(\frac{2\pi(\Phi - 0.5)}{L}\right)^2 + \left(\frac{\sqrt{2}\tilde{K}}{\sqrt{L}}\right)^2}. \quad (\text{A.5})$$

The equations are quite different for each parity as the sign of the ring-lead coupling depends on the parity as well.

For even parity, $\Phi \approx 0.5$ and weak coupling the source oscillations disappear in the weak-coupling limit. Interestingly, for even parity and strong coupling we still find density oscillations and we observe a characteristic beating. To calculate, we have to include in total four wavenumbers ($n = \frac{L}{4}$, $n = \frac{L+4}{4}$, and $n = \frac{3L}{4}$, $n = \frac{3L+4}{4}$) as at this flux all these ring modes have nearly the same energy. We get the same eigenvalues as in Eq.A.4 and additionally

$$E/J = 2 \sqrt{\sin\left(\frac{2\pi(\Phi - 1)}{L}\right)^2 + \left(\frac{\tilde{K}}{\sqrt{L}}\right)^2}. \quad (\text{A.6})$$

The beating frequency is given by the subtraction of these eigenvalues and Eq.A.4.

In the other limit $\Phi \approx 0$ and $K/J \approx 1$ or $L \gg 1$, a higher frequency mode appears in the density oscillation. To calculate, we include in total six wavenumbers ($n = \frac{L}{4}$, $n = \frac{L+4}{4}$, $n = \frac{L-4}{4}$, and $n = \frac{3L}{4}$, $n = \frac{3L+4}{4}$, $n = \frac{3L-4}{4}$). We get the original eigenvalue of Eq.A.4 and two new ones, of which only the

following has a non-negligible coefficient A_j

$$E/J = \left[\left(\frac{2\tilde{K}}{\sqrt{L}} \right)^2 + 2 \left(1 - \cos\left(\frac{4\pi}{L}\right) \cos\left(\frac{4\pi\Phi}{L}\right) \right) + \left\{ \left(\frac{2\tilde{K}}{\sqrt{L}} \right)^4 + \left(1 + \cos\left(\frac{8\pi}{L}\right) \cos\left(\frac{8\pi\Phi}{L}\right) - \cos\left(\frac{8\pi}{L}\right) - \cos\left(\frac{8\pi\Phi}{L}\right) \right\}^{\frac{1}{2}} \right]^{\frac{1}{2}}. \quad (\text{A.7})$$

This equation is not valid for small L and $\Phi \approx 0.5$.

Next, we show how to calculate off-resonant contributions. These are only present for odd parity, and do not play a role for even parity. In the weak-coupling limit, we assume that the eigenenergy E of the full system will be close to the energy of the uncoupled leads $E = 0$. This assumption is valid as the ring modes are far detuned from the leads. Thus, we perform a Taylor expansion of the fraction around $E = 0$

$$\frac{1}{\frac{E}{2J} + \cos\left(\frac{2\pi(n-\Phi)}{L}\right)} = \sum_{p=0}^{\infty} \left(-\frac{E}{2J} \right)^p \sec^{p+1}\left(\frac{2\pi(n-\Phi)}{L}\right).$$

The eigenvalue equation becomes

$$E\alpha_S = \frac{K^2}{2JL} \sum_{p=0}^{\infty} \left(\frac{-E}{2J} \right)^p (\beta_p^+ \alpha_S + \beta_p^- \alpha_D)$$

and analog for $E\alpha_D$. The symmetric and anti-symmetric combination of both equations give

$$E_{\pm} = \frac{K^2}{2JL} \sum_{p=0}^{\infty} \left(\frac{-E}{2J} \right)^p (\beta_p^+ \pm \beta_p^-)$$

We define

$$\beta_p^+ = \sum_{n=0}^{L-1} \sec\left(\frac{2\pi}{L}(n-\Phi)\right)^{p+1}$$

and

$$\beta_p^- = \sum_{n=0}^{L-1} (-1)^n \sec\left(\frac{2\pi}{L}(n-\Phi)\right)^{p+1}.$$

The coefficients reveal the parity effect in $L/2$. For even parity and all values of Φ , β_p^+ and β_p^- is zero or infinity for $p \in \text{even}$, which suppresses the oscillations. For the case $p \in \text{odd}$, β_p^+ and β_p^- have nearly the same absolute value. Here, we find that there is always an eigenvalue $E = 0$. The corresponding oscillation period between source and drain for this energy is $T \rightarrow \infty$. Thus, for even parity in $L/2$ off-resonant coupling can be neglected for any order of p . For odd parity in $L/2$, we have $\beta_p^+ = 0$ for $p \in \text{even}$ and $\beta_p^- = 0$ for $p \in \text{odd}$, else the coefficients are non-zero. Two exact solutions are known to us $\beta_0^- = \pm \frac{L}{2\cos(\Phi\pi)}$ and $\beta_1^+ = \frac{L^2}{2\cos(\Phi\pi)^2}$. For a simple zero order expansion of all modes, without resonant tunneling

(valid for $\Phi \approx 0$), the energy difference of symmetric and anti-symmetric mode and the oscillation frequency between drain and source is

$$E/J = \frac{\tilde{K}^2}{|\cos(\Phi\pi)|}. \quad (\text{A.8})$$

It is possible to also derive higher order versions of this equation for increased accuracy. First order yields

$$E/J = \frac{4\tilde{K}^2 \cos(\Phi\pi)}{8\cos(\Phi\pi)^2 + 2L\tilde{K}^2}. \quad (\text{A.9})$$

It is possible to combine resonant and off-resonant coupling. One has to apply the method for resonant coupling, and use the off-resonant method for all other eigenmodes minus the resonant ones. The sum over n has to be adjusted accordingly. The result for order $p = 0$ is

$$E_{\pm}/J = \pm \left[\frac{\tilde{K}^2}{2L \sin\left(\frac{\pi}{L}(1-2\Phi)\right)} - \frac{\tilde{K}^2}{4\cos(\Phi\pi)} + \sin\left(\frac{\pi}{L}(1-2\Phi)\right) \right] + \left[\left(\frac{\tilde{K}^2}{2L \sin\left(\frac{\pi}{L}(1-2\Phi)\right)} - \frac{\tilde{K}^2}{4\cos(\Phi\pi)} + \sin\left(\frac{\pi}{L}(1-2\Phi)\right) \right)^2 + \frac{\tilde{K}^2 \sin\left(\frac{\pi}{L}(1-2\Phi)\right)}{\cos(\pi\Phi)} \right]^{\frac{1}{2}}. \quad (\text{A.10})$$

and up to order $p = 1$ we get with $\delta = \csc\left(\frac{\pi}{L}(1-2\Phi)\right)$ and $\gamma = \sec(\Phi\pi)$

$$E_{\pm}/J = \pm \frac{L}{\delta} \frac{8 + \tilde{K}^2 L \gamma^2 - 2\tilde{K}^2 \delta \gamma}{4\tilde{K}^2 \delta^2 - L(8 + \tilde{K}^2 L \gamma^2)} + \left[\left(\frac{L}{\delta} \frac{8 + \tilde{K}^2 L \gamma^2 - 2\tilde{K}^2 \delta \gamma}{4\tilde{K}^2 \delta^2 - L(8 + \tilde{K}^2 L \gamma^2)} \right)^2 + \frac{L}{\delta} \frac{8\tilde{K}^2 \gamma}{8L + \tilde{K}^2(L^2 \gamma^2 - 4\delta^2)} \right]^{\frac{1}{2}}. \quad (\text{A.11})$$

Eq. A.11 describes the oscillation frequencies between source and drain for odd parity accurately over a wide parameter range.

So far, we only discussed the eigenvalues, which represent the frequency of the oscillation in source and drain. As outlined in the beginning of the section it can be described by a superposition of Cosines with the relevant eigenvalues of the reduced system. Now, we discuss the relative strength of the Cosine contribution A_{\pm} , which is the coefficient of the eigenvector in drain and source. For resonant coupling, we can write down the reduced Hamiltonian and solve for the eigenvectors and calculate A_j . For off-resonant coupling, writing down the reduced Hamiltonian is not so trivial. Using numerics, we established that for odd parity and $\Phi \approx 0$, E_+ dominates and only a minor contribution of E_- contributes for larger ring lengths. For $\Phi \approx 0.5$, both frequencies contribute equally, and a beating between the two frequencies occurs.

Comparison numerics and analytics

We plot the ring-lead coupling K for different U/J in Fig. 6. For weak-coupling K/J , we observe source drain oscillation

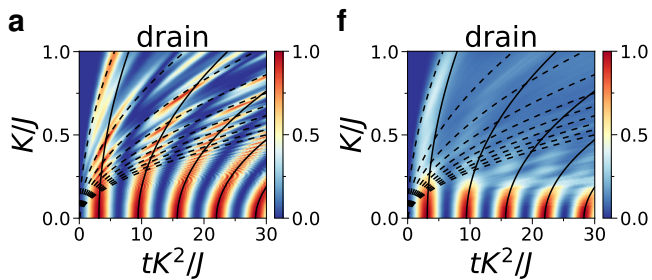


FIG. 6. Density in drain against K/J for $L/2 = 7$ and four particles with **a)** $U = 0$ and **b)** $U/J = 5$ with analytic solution using Eq.A.11. For weak ring-lead coupling only one oscillation mode contributes, whereas for strong coupling additional oscillation modes are excited.

which are nearly independent of U/J , as the ring population in the weak-coupling limit is low, suppressing particle-particle scattering. With increasing K/J , we notice faster oscillation patterns. They smear out with increasing interaction as the ring fills up for stronger ring-lead coupling.

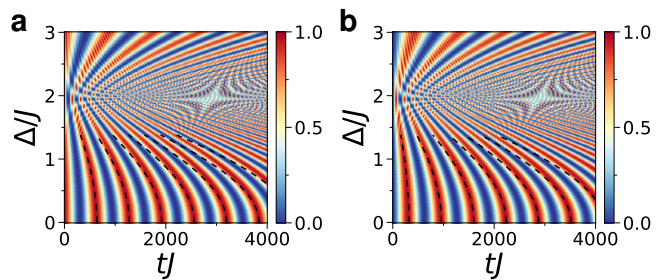


FIG. 7. Density in source and drain against two potential barriers in each arm of ring with potential depth Δ/J for **a,b)** $L/2 = 7$ without interaction $U = 0$. Other parameter are $K/J = 0.1$, $\Phi = 0$. The specific placement of the barriers has a strong impact on the dynamics. We choose a special placement which produced a behaviour which mimics the flux. The fit uses the formulas for flux, but replaces $\Phi = \Delta/(2J)$. The barriers behave like a scattering impurity, which couple different momentum modes. Δ mainly changes the frequency of the density oscillation, but does not add any new additional oscillation frequencies. This means that the system is still dominated by one eigenmode. The scattering is only perturbing the overall dynamics, but not adding higher frequencies (in contrast to increasing ring-lead coupling K or adding more ring sites).

Appendix: III. Applications

We show supplemental data for the first application: Inserting two potential barriers in the ring without interaction. By introducing two potential barriers Δ symmetrically in the center of upper and lower arm of the ring, we can mimic the effect of flux on the oscillation periods.

We plot the density in source and drain against Δ in Fig.7 without interaction $U = 0$. The oscillation frequency follows nearly the same relation as for flux, but no destructive interference is observed. This suggest we are not in the tunneling regime, and potential barriers and weak link play the role of scatters, and do not induce a simple phase shift.